



Article

Lightweight Designs and Improving the Load-Bearing Capacity of Structures by the Method of Aggregation

Michael Todinov



Article

Lightweight Designs and Improving the Load-Bearing Capacity of Structures by the Method of Aggregation

Michael Todinov

School of Engineering, Computing and Mathematics, Oxford Brookes University, Oxford OX33 1HX, UK; mtodinov@brookes.ac.uk

Abstract: The paper introduces a powerful method for developing lightweight designs and enhancing the load-bearing capacity of common structures. The method, referred to as the ‘method of aggregation’, has been derived from reverse engineering of sub-additive and super-additive algebraic inequalities. The essence of the proposed method is consolidating multiple elements loaded in bending into a reduced number of elements with larger cross sections but a smaller total volume of material. This procedure yields a huge reduction in material usage and is the first major contribution of the paper. For instance, when aggregating eight load-carrying beams into two beams supporting the same total load, the material reduction was more than 1.58 times. The second major contribution of the paper is in demonstrating that consolidating multiple elements loaded in bending into a reduced number of elements with larger cross sections but the same total volume of material leads to a big increase in the load-bearing capacity of the structure. For instance, when aggregating eight cantilevered or simply supported beams into two beams with the same volume of material, the load-bearing capacity until a specified tensile stress increased twice. At the same time, the load-bearing capacity until a specified deflection increased four times.

Keywords: method of aggregation; algebraic inequality; lightweight design; load-bearing capacity; cantilevered beams; simply supported beams

MSC: 39B62



Citation: Todinov, M. Lightweight Designs and Improving the Load-Bearing Capacity of Structures by the Method of Aggregation. *Mathematics* **2024**, *12*, 1522. <https://doi.org/10.3390/math12101522>

Academic Editor: Manuel Pastor

Received: 16 April 2024

Revised: 5 May 2024

Accepted: 9 May 2024

Published: 14 May 2024



Copyright: © 2024 by the author. Licensee MDPI, Basel, Switzerland. This article is an open access article distributed under the terms and conditions of the Creative Commons Attribution (CC BY) license (<https://creativecommons.org/licenses/by/4.0/>).

1. Introduction

Algebraic inequalities play a crucial role in various mathematical applications, serving to establish bounds, estimate errors, and various upper and lower bounds [1–7]. The comprehensive exploration of methods for proving algebraic inequalities is well documented [7–9], and in the domain of engineering, the application of algebraic inequalities has primarily focused on specifying design constraints [10–15].

However, there has been a notable absence of attempts to use algebraic inequalities for a direct generation of new knowledge and optimization of systems and processes through a physical interpretation of the variables and the different terms building the inequalities. A recent development featuring this approach was referred to as the *reverse engineering of algebraic inequalities* [16].

Sub-additive and super-additive algebraic inequalities, the properties of which have been discussed in the literature [17], are excellent candidates for reverse engineering. Power laws are ubiquitous in describing physical phenomena; therefore, sub-additive and super-additive algebraic inequalities based on power laws are likely the best candidates for reverse engineering. Several relevant examples of such reverse engineering have already been presented [16].

Lightweight components can be obtained through design, manufacturing, and lightweight materials. A major trend in lightweight parts obtained through design is the simulation-driven design technique known as ‘topology optimization’ [18,19]. In addition, lightweight

components can also be obtained using advanced manufacturing technologies such as advanced metal forming [20] and additive manufacturing [21,22].

There is, however, another powerful yet overlooked method for improving the load-bearing capacity of structures and producing lightweight structures. This method will be referred to as *the method of aggregation* and was discovered through reverse engineering of algebraic inequalities. Accordingly, this paper demonstrates huge material savings and increase of the load-carrying capacity of structures obtained through the method of aggregation. As a result, the method of aggregation is directly related to structural design.

For multiple, uniformly loaded identical elements, we can distinguish two alternative arrangements: a non-aggregated structure, composed of n loaded in bending elements, and an aggregated structure composed of a smaller number m of loaded in bending elements with larger cross-sections. As shall be demonstrated later, aggregating loaded in bending elements into fewer loaded elements with larger cross-sections opens a huge opportunity for material saving. Despite the widespread use of multiple load-carrying elements in engineering and construction, there is a surprising deficiency in the analysis of non-aggregated and aggregated structures. Notably, standard textbooks on stress analysis and machine design [23–27] lack a key discussion. This is related to the comparison of the total volume of material needed to support a load of specified magnitude for alternative structures based on varying numbers of load-carrying elements. Similarly, no analysis is present related to the load-carrying capacity of non-aggregated and aggregated structure built with the same volume of material. Surprisingly, this critical discussion is absent not only in textbooks dedicated to structural engineering [28,29] but also in the structural reliability literature [30,31] and in papers focusing on the optimization of loaded beams [32,33].

2. Sub-Additive and Super-Additive Inequalities Based on a Concave and Convex Power Law Dependence

Consider the sub-additive inequality:

$$ax_1^p + ax_2^p + \dots + ax_m^p < ay_1^p + ay_2^p + \dots + ay_n^p \tag{1}$$

where $m < n$, $p < 1$, $x_i > 0$, $y_i > 0$, $a > 0$ and $\sum_{i=1}^m x_i = \sum_{i=1}^n y_i$. In general, inequality (1) holds under the following sufficient majorizing conditions:

$$\begin{aligned} x_1 &\geq y_1; x_1 \geq y_2; \dots; x_1 \geq y_n \\ x_2 &\geq y_1; x_2 \geq y_2; \dots; x_2 \geq y_n \\ x_m &\geq y_1; x_m \geq y_2; \dots; x_m \geq y_n \end{aligned} \tag{2}$$

The majorizing conditions (2) effectively state that any x_i in the left-hand side of inequality (1) majorizes each y_i in the right-hand side of the inequality. (In general, x_i and y_i are not necessarily equal). The proof of inequality (1) under these sufficient conditions has been given in Appendix A.

For equal x_i and y_i ($x_1 = x_2 = \dots = x_m = z/m$ and $y_1 = y_2 = \dots = y_n = z/n$), the sufficient majorizing conditions (2) are automatically satisfied, and inequality (1) holds true. For this important special case, however, a simplified proof of the inequality can be given, which is presented in Appendix B.

For $p > 1$, $m < n$, $x_i > 0$, $y_i > 0$, $a > 0$, $\sum_{i=1}^m x_i = \sum_{i=1}^n y_i$ and under the same sufficient conditions (2) specified for inequality (1), it can be proved that the super-additive inequality

$$ax_1^p + ax_2^p + \dots + ax_m^p > ay_1^p + ay_2^p + \dots + ay_n^p \tag{3}$$

holds true. (The details of the proof are similar to those related to inequality (1) and are omitted here).

The primary advantage of inequalities (1) and (3) lies in their simplicity and ease of physical interpretation, which renders them particularly suitable for reverse engineering.

In inequalities (1) and (3), x and y can be interpreted as additive quantities, while ‘ a ’ and ‘ p ’ are constants. The additive quantities increase with the expansion of the system’s size. Examples of additive quantities include force, mass, volume, length, kinetic energy, potential energy, elastic energy, work, electric current, heat, and enthalpy. For a meaningful physical interpretation of inequalities (1) and (3), each individual term ax_i^p and ay_i^p within the inequalities must also be an additive quantity.

Inequality (1) can be physically interpreted if the variables x_i and y_i are interpreted as load magnitudes for an element loaded in bending. The terms ax_i^p and ay_i^p in (1) can be interpreted as the minimal volume of material necessary to support bending loads of magnitudes x_i and y_i , where $P = \sum_{i=1}^m x_i = \sum_{i=1}^n y_i$ is the total bending load carried by each structure. Consequently, the left-hand side of inequality (1) represents the minimal volume of a structure built with m elements loaded in bending, necessary to carry a total load $P = \sum_{i=1}^m x_i$. The right-hand side of the inequality represents the minimal volume of an alternative structure built with n elements loaded in bending, necessary to carry the same total load $P = \sum_{i=1}^n y_i$. As a result, the physical interpretation of inequality (1) provides a mechanism for comparing the volumes of material needed for the competing structures loaded in bending and selecting the alternative characterized by the smaller volume of material.

Just as the reverse engineering of the sub-additive inequality (1) compares the minimum volumes of material necessary to carry the same total bending load, the reverse engineering of the super-additive inequality (3) compares the load-bearing capacities at the same total volume of material for building the structures loaded in bending. To achieve this, the variables x_i and y_i are physically interpreted as ‘volumes of the elements loaded in bending, building the structures’. The terms ax_i^p and ay_i^p in (3) can be physically interpreted as ‘the bending loads supported by the individual elements of the structure’ whose volumes are x_i and y_i , respectively. In this case, the volume of material used for each of the competing structures is the same: $V = \sum_{i=1}^m x_i = \sum_{i=1}^n y_i$. As a result, the left-hand side of the super-additive inequality (3) represents the total bending load P_1 carried by a structure built with m elements loaded in bending: $P_1 = \sum_{i=1}^m ax_i$. The right-hand side of inequality (3) represents the total bending load P_2 carried by an alternative structure built with the same total volume of material, which includes n elements loaded in bending: $P_2 = \sum_{i=1}^n ay_i$. The physical interpretation of inequality (3) provides a mechanism for comparing the load-bearing capacities of competing structures loaded in bending, at the same volume of material used for building the structures. In summary, the proposed inequalities (1) and (3) provide the theoretical basis for the method of aggregation in developing lightweight designs and increasing the load-bearing capacity of structures under bending loads.

Despite the fact that the inequalities (1) and (3) are applicable to non-uniform loads and cross-sections, the paper illustrates the power of the aggregation method by focusing on uniformly distributed loads and uniform cross-sections of load-bearing elements. This choice is deliberate for several reasons. Firstly, the uniform distribution automatically fulfils the majorizing conditions (2), sufficient for the validity of inequalities (1) and (3). Secondly, it encompasses an important special case with practical importance. Thirdly, it makes it possible to easily quantify the effects of applying aggregation. Lastly, the uniform setup allows for a straightforward treatment, facilitating a better understanding of the aggregation method.

3. Alternative Structures Loaded in Bending Based on Cantilevered Beams

Consider two alternative structures, each including m and n identical load-bearing beams, correspondingly, where $m < n$ (Figure 1a,b). The length L of the beams is the same for both structures. The aggregated structure (Figure 1a) differs from the non-aggregated structure (Figure 1b) in that it contains fewer cantilevered beams with larger cross-sections. For the sake of simplicity of the derivations and presentation, the variations in material properties and geometry were not considered.

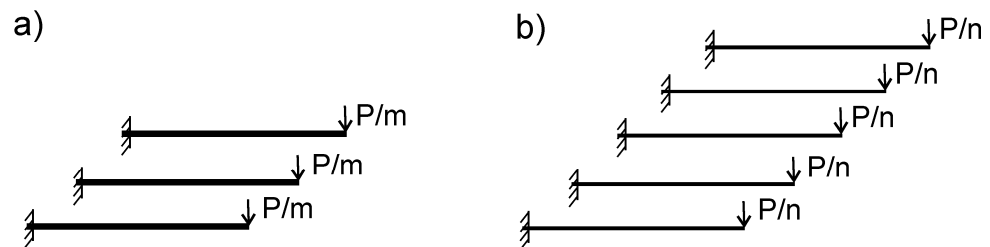


Figure 1. (a) Aggregated and (b) non-aggregated structure based on cantilever beams.

3.1. Minimum Volume of Material Needed for Supporting a Total Bending Load of a Specified Magnitude

Suppose that the critical tensile stress permitted by the material of both structures in Figure 1 is σ_{cr} . Consider a uniform distribution of the bending load P over the load-bearing beams. In this case, the bending loads per beam for the aggregated and non-aggregated structure are P/m and P/n , respectively. We will calculate the minimum necessary volume of material for the aggregated structure (Figure 1a) and the non-aggregated structure (Figure 1b), needed to support a total bending load of given magnitude P .

For a cantilevered beam with radius r of the cross section, subjected to a bending moment M , the absolute value of the maximum stress σ is given by the familiar expression [27]:

$$\sigma = (M/I)r \tag{4}$$

where I is the second moment of area of the circular cross section. Since for a circular cross section, $I = \pi r^4/4$, expression (4), solved with respect to the radius r , gives:

$$r = [4M/(\pi\sigma)]^{1/3}$$

The loading moment at the fixed end of a cantilevered beam from the aggregated structure in Figure 1a is $(P/m) \times L$ and for the non-aggregated structure in Figure 1b, the loading moment is $(P/n) \times L$. Assume that the same permissible critical tensile stress σ_{cr} is developed in the beams from both structures. Then, for the radius r_1 of the load-bearing beams from the aggregated structure, the expression:

$$r_1 = [4PL/(m\pi\sigma_{cr})]^{1/3}$$

is obtained while for the radius r_2 of the load-bearing beams of the non-aggregated structure, the expression:

$$r_2 = [4PL/(n\pi\sigma_{cr})]^{1/3}$$

is obtained. The volume of a single beam from the aggregated structure is therefore given by:

$$v_1 = \pi r_1^2 L = \pi L [4PL/(m\pi\sigma_{cr})]^{2/3} = \pi L [4L/(\pi\sigma_{cr})]^{2/3} \times [P/m]^{2/3} \tag{5}$$

while the volume of a single beam from the non-aggregated structure is given by:

$$v_2 = \pi r_2^2 L = \pi L [4PL/(n\pi\sigma_{cr})]^{2/3} = \pi L [4L/(\pi\sigma_{cr})]^{2/3} \times (P/n)^{2/3}$$

If we denote $x_i = P/m, y_i = P/n, (\sum_{i=1}^m x_i = \sum_{i=1}^n y_i = P)$ and $a = \pi L[4L/(\pi\sigma_{cr})]^{2/3}$, the majorizing conditions (2) for inequality (1) will be fulfilled and it becomes:

$$ax_1^{2/3} + \dots + ax_m^{2/3} < ay_1^{2/3} + \dots + ay_n^{2/3} \tag{6}$$

The physical interpretation of inequality (6) then yields the following. The total volume $V_1 = ax_1^{2/3} + ax_2^{2/3} + \dots + ax_m^{2/3}$ of the beams in the aggregated structure needed to support the total load P is smaller than the total volume $V_2 = ay_1^{2/3} + ay_2^{2/3} + \dots + ay_n^{2/3}$ of the beams in the non-aggregated structure needed to support the same total load P . Considering that the left-hand side of (6) is equal to $V_1 = ma(P/m)^{2/3}$ and the right-hand side of (6) is equal to $V_2 = na(P/n)^{2/3}$, the ratio of the two volumes is given by:

$$V_2/V_1 = (n/m)^{1/3} \tag{7}$$

The material saving given by Equation (7) is very big. According to Equation (7), for $m = 1$, the material saving factor s_f is given by the expression:

$$s_f = n^{1/3} \tag{8}$$

where n is the number of load-carrying beams in the non-aggregated structure. Evaluating expression (8), for $n = 2, 3, 4, 5, 6, \dots$, yields the material saving factors $s_f = 1.26, 1.44, 1.587, 1.71, 1.82 \dots$. These indicate that applying the method of aggregation yields huge material savings.

3.2. Comparison and Verification

For the purposes of the comparison and verification of these theoretical results, the following three variants of aggregation were analysed. First, two cylindrical cantilevered beams supporting a specified total bending load P were considered, aggregated into a single cylindrical cantilevered beam with a $2^{1/3}$ times smaller volume, supporting the same total bending load, P (Figure 2a). Next, three beams supporting a specified total load P were considered, aggregated into a single cantilevered beam with a $3^{1/3}$ times smaller volume, supporting the same total bending load P (Figure 2b). Finally, four beams supporting a specified total load P were considered, aggregated into a single beam with a $4^{1/3}$ times smaller volume carrying the same total bending load P (Figure 2c).

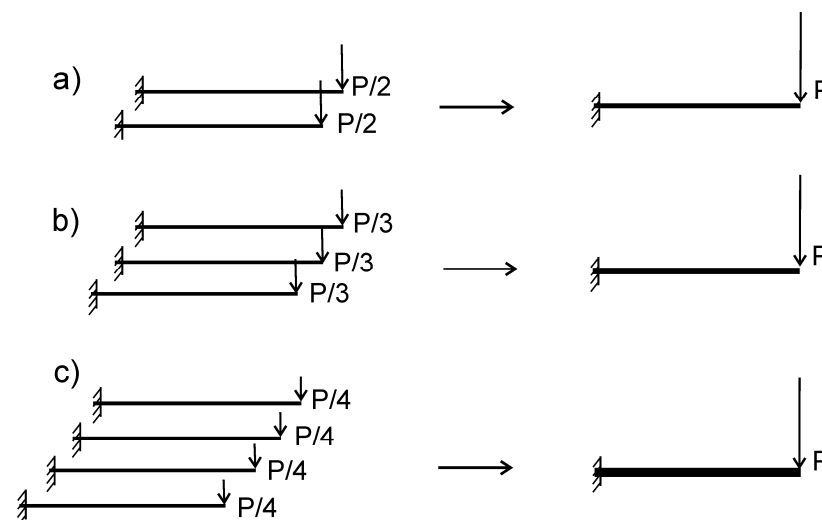


Figure 2. (a) Two-to-one, (b) three-to-one, and (c) four-to-one aggregation of cantilever beams.

In the first variant of aggregation, the non-aggregated system is composed of two cylindrical cantilevered beams with lengths $L = 0.3$ m and radii $r_1 = r_2 = 6$ mm, each loaded with a force $P/2 = 90$ N. The total force is therefore $P = 180$ N (Figure 2a).

The combined cross-sectional area of the non-aggregated system is therefore $\pi r_1^2 + \pi r_2^2 = 226.19$ mm².

The aggregated system is a single beam with the same length L and a reduced cross-sectional area with the factor $2^{1/3}$ (1.26). It carries the same total load of 180 N (Figure 2a). Therefore, for the cross-sectional area of the aggregated beam, we have $\pi R^2 = 226.19/2^{1/3}$, from which:

$$R = \sqrt{226.19/(2^{1/3} \times \pi)} = 7.559 \text{ mm} \tag{9}$$

where R is the radius of the single aggregated beam.

In the second variant of aggregation, the non-aggregated system is composed of three cylindrical cantilevered beams with lengths $L = 0.3$ m and radii $r_1 = r_2 = r_3 = 6$ mm, each loaded with a force $180/3 = 60$ N (Figure 2b). The total loading force is $P = 180$ N, and the combined cross-sectional area of the non-aggregated system is $\pi r_1^2 + \pi r_2^2 + \pi r_3^2 = 339.292$ mm². The aggregated system is a single beam with the same length L and a reduced cross-sectional area with the factor $3^{1/3}$ (1.44). It supports the same total load of 180 N (Figure 2b). Therefore, for the cross-sectional area of the single beam we have: $\pi R^2 = 339.292/3^{1/3}$, from which:

$$R = \sqrt{339.292/(3^{1/3} \times \pi)} = 8.653 \text{ mm}, \tag{10}$$

where R is the radius of the single aggregated beam.

In the third variant of aggregation, the non-aggregated system is composed of four cylindrical cantilevered beams with lengths $L = 0.3$ m and radii $r_1 = r_2 = r_3 = r_4 = 6$ mm, each loaded with a force $180/4 = 45$ N (Figure 2c). The total loading force is therefore again $P = 180$ N. The combined cross-sectional area of the non-aggregated system is $\pi r_1^2 + \pi r_2^2 + \pi r_3^2 + \pi r_4^2 = 452.389$ mm². The aggregated system is a single beam which carries the same load of 180 N, has the same length L , and has a reduced cross-sectional area with the factor $4^{1/3}$ (1.587). Therefore, $\pi R^2 = 452.389/4^{1/3}$, from which:

$$R = \sqrt{452.389/(4^{1/3} \times \pi)} = 9.524 \text{ mm} \tag{11}$$

is obtained, where R is the radius of the single aggregated beam.

The maximum tensile stress from loading the cantilevered beams has been calculated using the classical stress analysis Formula (4) for simple bending, and the results are listed in Table 1. As can be seen from the table, *the maximum tensile stress is the same for the aggregated and non-aggregated structures, which demonstrates that at the same maximum tensile stress, the aggregated structure can support the same total load with a much smaller volume of material.* The material-saving factor s_f is given by Equation (8).

Table 1. Results for the maximum tensile stress for the non-aggregated and aggregated cantilever beams.

	Non-Aggregated	Aggregated
Two-to-one	159.2 MPa	159.2 MPa
Three-to-one	106.1 MPa	106.1 MPa
Four-to-one	79.6 MPa	79.6 MPa

3.3. Load-Bearing Capacity Comparison between Two Cantilevered Structures Built with the Same Total Volume of Material

Consider again two alternative structures, each including m and n identical load-bearing beams, correspondingly, where $m < n$ and the length L of the beams in both structures is the same. The cross-sectional area of each beam from the first (aggregated)

structure is S_1 while the cross-sectional area of each beam from the second (non-aggregated) structure is S_2 and $S_1 > S_2$. This means that the aggregated structure has been obtained from the non-aggregated structure by consolidating the beams into fewer beams with larger cross sections (Figure 1a). In addition, the volume of material for both structures is the same, which means that the relationship

$$mS_1L = nS_2L \tag{12}$$

holds, from which:

$$S_1/S_2 = n/m \tag{13}$$

If the radius of the load-bearing beams from the aggregated structure is r_1 and that for the non-aggregated structure is r_2 , from Equation (13), it follows that:

$$r_1/r_2 = \sqrt{n/m} \tag{14}$$

Suppose that the maximum tensile stress permitted by the material of the beams is σ_{cr} . Let P_1 denote the total load the aggregated structure can support to a critical stress of magnitude σ_{cr} . Let P_2 denote the total load that the non-aggregated structure can sustain to a critical stress of magnitude σ_{cr} . It is assumed that the beams are loaded uniformly, which means that each beam from the aggregated structure supports a load of magnitude P_1/m , while the beams from the non-aggregated structure support a load of magnitude P_2/n .

Let us compare the load-bearing capacities of the aggregated and non-aggregated structure *built with the same total volume of material*. Since for a circular cross section, the second moment of area is $I = \pi r^4/4$, expression (4) yields:

$$\sigma = 4M/(\pi r^3) = 4PL/(\pi r^3) \tag{15}$$

where P is the loading force and L is the length of the cantilever beam. If $\sigma = \sigma_{cr}$ is set in (15) and the equation is solved with respect to the loading force P , an expression for the maximum loading force that sets a critical tensile stress of magnitude σ_{cr} is obtained:

$$P = \sigma_{cr}\pi r^3/(4L) \tag{16}$$

Let P_1 be the maximum total load that the aggregated structure composed of m beams with radii r_1 can support. Since the loading per beam from the aggregated structure is P_1/m , substituting in (16) gives:

$$P_1/m = \sigma_{cr}\pi r_1^3/(4L) \tag{17}$$

Similarly, let P_2 be the maximum total load that the non-aggregated structure composed of n beams with radii r_2 can support. Since the loading per beam from the non-aggregated structure is P_2/n , substituting in (16) gives:

$$P_2/n = \sigma_{cr}\pi r_2^3/(4L) \tag{18}$$

Let $x_1 = x_2 = \dots = x_m = (\pi r_1^2 L)$ stand for the volumes of the load-bearing beams from the aggregated structure and $y_1 = y_2 = \dots = y_n = (\pi r_2^2 L)$ stand for the volumes of the load-bearing beams from the non-aggregated structure. Equation (17) can then be written as:

$$P_1/m = [\pi\sigma_{cr}/(4L)] \times [x_1^{3/2}/(\pi^{3/2}L^{3/2})]$$

while Equation (18) can be written as:

$$P_2/n = [\pi\sigma_{cr}/(4L)] \times [y_1^{3/2}/(\pi^{3/2}L^{3/2})]$$

Next, denote $a_1 = \dots = a_m = \dots = a_n = a = \pi\sigma_{cr}/(4L\pi^{3/2}L^{3/2})$. The sufficient conditions (2) for the super-additive inequality (3) are then fulfilled and according to inequality (3):

$$ax_1^{3/2} + \dots + ax_m^{3/2} > ay_1^{3/2} + \dots + ay_n^{3/2} \tag{19}$$

The left-hand side of inequality (19), $P_1 = ax_1^{3/2} + \dots + ax_m^{3/2}$, is the total bending load supported by the aggregated structure, while the right-hand side, $P_2 = ay_1^{3/2} + \dots + ay_n^{3/2}$, is the total bending load supported by the non-aggregated structure. Considering that the left-hand side of (19) is equal to $P_1 = ma(\pi r_1^2 L)^{3/2}$ and the right-hand side is equal to $P_2 = na(\pi r_2^2 L)^{3/2}$, the ratio of the two forces can be obtained:

$$P_1/P_2 = (m/n) \times (r_1/r_2)^3$$

Since the volume of material used for building both structures is the same, from Equation (14), it follows that:

$$(r_1/r_2)^3 = (n/m)^{3/2}$$

and the ratio P_1/P_2 of the load-bearing capacities of the aggregated and non-aggregated structure becomes:

$$P_1/P_2 = (m/n) \times (n/m)^{3/2} = \sqrt{n/m} \tag{20}$$

For $m = 2$ and $n = 8$, for example, this ratio is $P_1/P_2 = 2$ which demonstrates that for the same total volume of the load-bearing beams in the two structures, the aggregated structure (Figure 1a) has a significantly larger load-bearing capacity than the non-aggregated structure.

3.4. Load-Bearing Capacities at the Same Maximum Permissible Deflection of Two Cantilevered Structures Built with the Same Total Volume of Material

Suppose now that the limiting condition during loading is not the maximum permissible tensile stress but the maximum permissible deflection δ_{cr} . Let the loads that the aggregated and non-aggregated structures can support at a critical deflection of magnitude δ_{cr} be P_1 and P_2 , correspondingly. The load-bearing beams are loaded uniformly. This means that each beam from the aggregated structure supports a load of magnitude P_1/m while each beam from the non-aggregated structure supports a load of magnitude P_2/n .

Because the volume of material for both structures is the same, the ratio of the radii is given by Equation (14). For a cantilever beam, the link between a deflection of magnitude δ_{cr} and the loading force P that causes this deflection is given by the classical formula [27]:

$$\delta_{cr} = PL^3/(3EI) \tag{21}$$

where E is the Young's modulus of the material and I is the second moment of area. Solving (21) for P gives:

$$P = 3EI\delta_{cr}/L^3 \tag{22}$$

Considering that for a circular section, $I = \pi r^4/4$, Equation (22) becomes:

$$P = 3E\pi r^4\delta_{cr}/(4L^3) \tag{23}$$

Since each beam from the aggregated structure has a radius r_1 and is loaded by a force P_1/m , for a single beam from the aggregated structure, the following relationship holds:

$$P_1/m = 3E\pi r_1^4\delta_{cr}/(4L^3) \tag{24}$$

For the non-aggregated structure, each beam has a radius r_2 and is loaded by a force P_2/n . Therefore, for a single beam from the non-aggregated structure, the corresponding relationship is:

$$P_2/n = 3E\pi r_2^4 \delta_{cr} / (4L^3) \tag{25}$$

It can be shown that the inequality: $P_1 > P_2$ holds if $n > m$. Indeed, taking the ratio of (24) and (25) gives

$$P_1 n / (P_2 m) = r_1^4 / r_2^4 \tag{26}$$

From relationship (14), $r_1^4 / r_2^4 = n^2 / m^2$ is obtained and the substitution in (26) gives:

$$P_1 n / (P_2 m) = r_1^4 / r_2^4 = n^2 / m^2$$

from which:

$$P_1 / P_2 = n / m \tag{27}$$

Again, the aggregation of the cross sections led to an increased load-carrying capacity of the aggregated structure despite that both structures are built with the same volume of material. For $n = 8, m = 2$, for example, the aggregated structure has four times greater load-bearing capacity compared to the non-aggregated structure:

$$P_1 / P_2 = n / m = 4 \tag{28}$$

Although the load per beam increases in the aggregated structure, this is outweighed by the increase in the second moment of area of the cross section. For cantilevered beams, the deformation is given by Equation (21). Despite the increase of the load P in the numerator from aggregating the loads, this increase is outweighed by the more significant increase of the second moment of area 'I' of the cross sections, caused by the increased radius r . Indeed, the second moment of area depends on the fourth power of the radius of the beam ($I = \pi r^4 / 4$).

The aggregation method can indeed be derived by bypassing the sub-additive and super-additive inequalities (1) and (3). However, this can only be accomplished for uniform loading and uniform cross sections. In cases of a non-uniform loading and non-uniform cross sections, the general form of inequalities (1) and (3) must be used. It is not clear how the result related to non-uniform loading or non-uniform cross sections can be derived by bypassing the inequalities (1) and (3).

4. Structures Built on Simply Supported Beams

Consider now two alternative structures including m and n load-bearing simply supported beams, correspondingly, where $m < n$ (Figure 3a,b). Again, the length L of the beams in both structures is the same. The structure in Figure 3a, consisting of fewer (m) load-bearing beams with larger cross-sectional area, will be referred to as the 'aggregated' structure, while the structure in Figure 3b, consisting of a larger number (n) of load-bearing beams with smaller cross-sectional area, will be referred to as the 'non-aggregated' structure.

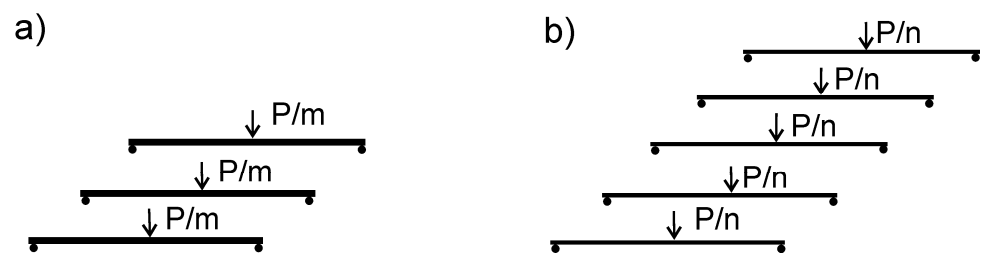


Figure 3. (a) Aggregated and (b) non-aggregated structure built on simply supported beams.

4.1. Minimum Volume of Material Needed to Carry a Load of a Specified Magnitude P

Similar to the case of the cantilevered beams, suppose that σ_{cr} is the maximum permissible stress of the material for the structures in Figure 3. Assume a uniform distribution of the load over the load-bearing beams. The loads per beam for the aggregated and non-aggregated structures are P/m and P/n , respectively.

Using a very similar reasoning to the reasoning in Section 3.2 related to cantilevered beams (which will not be repeated here), the ratio of the volumes of aggregated and non-aggregated structures necessary to support a total load of magnitude P can be determined. The ratio of the minimum volumes necessary to support a total load of magnitude P is again given by the expression (7) ($V_1/V_2 = (n/m)^{1/3}$), and for $m = 1$, the material-saving factor $s_f = V_1/V_2 = n^{1/3}$ is given by expression (8). Again, the total volume V_1 of the load-bearing beams of the aggregated structure needed to support the total load P is significantly smaller than the total volume V_2 of the load-bearing beams of the non-aggregated structure needed to support the same total load P .

4.2. Comparison and Verification

The comparison of structures involving simply supported beams also involves three types of aggregation. First, two beams carrying a total load P were considered, aggregated into a single beam with the same length L and with a $2^{1/3}$ times smaller volume, carrying the same total load P (Figure 4a). Next, three beams carrying a total load P were considered, aggregated into a single beam with the same length L and a $3^{1/3}$ times smaller volume supporting the same total load P (Figure 4b). Finally, four beams carrying a specified total load P were considered, aggregated into a single beam with the same length L and a $4^{1/3}$ times smaller volume, supporting the total load P (Figure 4c).

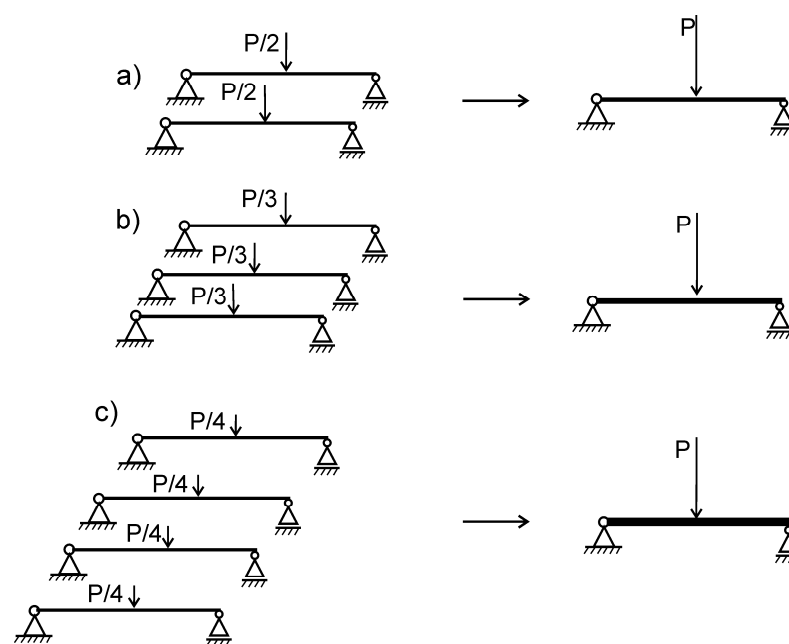


Figure 4. (a) Two-to-one, (b) three-to-one, and (c) four-to-one aggregation of simply supported beams.

In the first variant of aggregation (Figure 4a), the non-aggregated structure was composed of two simply supported cylindrical rods with lengths $L = 0.8$ m and radii $r_1 = r_2 = 6$ mm, each loaded with a force $P/2 = 180$ N. The total force was therefore $P = 360$ N. The aggregated beam had the same length L , a reduced cross-sectional area with the factor $2^{1/3}$ (1.26), and it supported the same total load of 360 N. The radius $R = 7.559$ mm of the single aggregated beam was calculated with Equation (9), which was also used for calculating the cross section of the aggregated cantilever beam.

In the second variant of aggregation (Figure 4b), the non-aggregated structure was composed of three simply supported beams with lengths $L = 0.8$ m and radii $r_1 = r_2 = r_3 = 6$ mm, each loaded with a force $360/3 = 120$ N. The total loading force was therefore again $P = 360$ N. The radius $R = 8.653$ mm of the single aggregated beam was calculated using Equation (10), which was also used for calculating the cross section of the aggregated cantilever beam.

Finally, in the third variant of aggregation (Figure 4c), the non-aggregated system was composed of four cylindrical simply supported beams with lengths $L = 0.8$ m and radii $r_1 = r_2 = r_3 = r_4 = 6$ mm, each loaded with a force $360/4 = 90$ N. The total loading force was therefore $P = 360$ N. The radius $R = 9.524$ mm of the single aggregated beam was calculated using Equation (11), which was also used for calculating the cross section of the aggregated cantilever beam. The maximum tensile stress from loading the simply supported structures has been calculated using the standard stress analysis Formula (4) for simple bending, and the results are listed in Table 2.

Table 2. Maximum tensile stress for the non-aggregated and aggregated simply supported beams.

	Non-Aggregated	Aggregated
Two-to-one	212.2 MPa	212.2 MPa
Three-to-one	141.5 MPa	141.5 MPa
Four-to-one	106.1 MPa	106.1 MPa

As can be seen from Table 2, the maximum tensile stress is the same for the aggregated and non-aggregated structures. This demonstrates that at the same maximum tensile stress, the aggregated structure can support the same total load P with a much smaller volume of material compared to the non-aggregated structure.

4.3. Load-Bearing Capacity for Simply Supported Beam Structures Built with the Same Total Volume of Material

Suppose that the permissible stress of the material for the beams is σ_{cr} . Let P_1 be the load that the aggregated structure can support, which corresponds to the permissible stress σ_{cr} . Let P_2 be the load that the non-aggregated structure can support, which corresponds to the permissible stress σ_{cr} . Suppose also that the simply supported beams are loaded uniformly. This means that each beam from the aggregated structure in Figure 3a carries load of magnitude P_1/m , while each beam from the non-aggregated structure in Figure 3b carries load of magnitude P_2/n . Using a very similar reasoning to the reasoning in Section 3.2 related to cantilevered beams (which will not be repeated here), the ratio of the load-bearing capacities of the aggregated and non-aggregated structure at the same total volume of material used for building the structures can be determined. The ratio is given with the equation:

$$P_1/P_2 = \sqrt{n/m} \tag{29}$$

which is the same equation as the one derived for cantilevered beams. For $m = 2$ and $n = 8$, for example, Equation (29) gives $P_1/P_2 = 2$. Again, for the same total volume of the load-bearing beams in the two structures, the aggregated structure (Figure 3a) has a load-bearing capacity two times larger than that of the non-aggregated structure (Figure 3b).

4.4. Load-Bearing Capacity at the Same Maximum Permissible Deflection for Structures Built with the Same Total Volume of Material

Suppose that the limiting condition for the loading is not the maximum tensile stress but the maximum permissible deflection. Let the maximum permissible deflection δ_{cr} be the same for both the non-aggregated and aggregated structures. Suppose that P_1 is the total load on the aggregated structure in Figure 3a that corresponds to a maximum permissible deflection of magnitude δ_{cr} . Suppose that P_2 is the total load on the non-aggregated structure in Figure 3b that corresponds to a maximum permissible deflection

of magnitude δ_{cr} . It is assumed again that the load-bearing beams are loaded uniformly. This means that each beam from the aggregated structure in Figure 3a carries load of magnitude P_1/m , while each beam from the non-aggregated structure in Figure 3b carries load of magnitude P_2/n . Because the volume of material for both structures is the same, the ratio of the radii of the beams is given by Equation (14).

The link between the maximum permissible deflection δ_{cr} and the loading force P that causes this deflection for a simply supported beam is given by [27]:

$$\delta_{cr} = PL^3 / (48EI)$$

from which

$$P = 48EI\delta_{cr} / L^3 \tag{30}$$

Considering that for a circular section, $I = \pi r^4 / 4$, Equation (30) becomes:

$$P = 12E\pi r^4 \delta_{cr} / L^3 \tag{31}$$

Each beam from the aggregated structure in Figure 3a has a radius r_1 and is loaded by a force P_1/m . Therefore, for a single beam from the aggregated structure, the following relationship holds:

$$P_1/m = 12E\pi r_1^4 \delta_{cr} / L^3 \tag{32}$$

Similarly, each beam from the non-aggregated structure in Figure 3b has a radius r_2 and is loaded by a force P_2/n . Therefore, for a single beam from the non-aggregated structure, the relationship is:

$$P_2/n = 12E\pi r_2^4 \delta_{cr} / L^3 \tag{33}$$

Taking the ratio of (32) and (33) gives:

$$P_1 n / (P_2 m) = r_1^4 / r_2^4 \tag{34}$$

From relationship (14), $r_1^4 / r_2^4 = n^2 / m^2$ and the substitution in (34) gives:

$$P_1 n / P_2 m = r_1^4 / r_2^4 = n^2 / m^2$$

or the ratio of the load-bearing capacities becomes:

$$P_1 / P_2 = n / m \tag{35}$$

This result is identical with the ratio of the load-bearing capacities (27) obtained for structures built on cantilevered beams. The aggregation of the cross sections of simply supported beams leads to an increased load-bearing capacity of the structure at the same volume of material.

5. Load-Bearing Capacity Comparison between Γ -Frames Built with the Same Total Volume of Material

The Γ -frames are examples of more complex elements loaded in bending. The type of aggregation selected for the Γ -frames was also eight to two. The next example features a non-aggregated structure containing eight load-bearing elements (Figure 5a) with diameter of the wire $\phi 1$ mm which was aggregated into a structure containing only two load-bearing elements with diameters of the wires $\phi 2$ mm (Figure 5b). The other dimensions of the Γ -frames are presented in Figure 5. The diameters of the Γ -frames from the aggregated and non-aggregated structure were selected such that the volumes of material used for the aggregated and non-aggregated structures were the same.

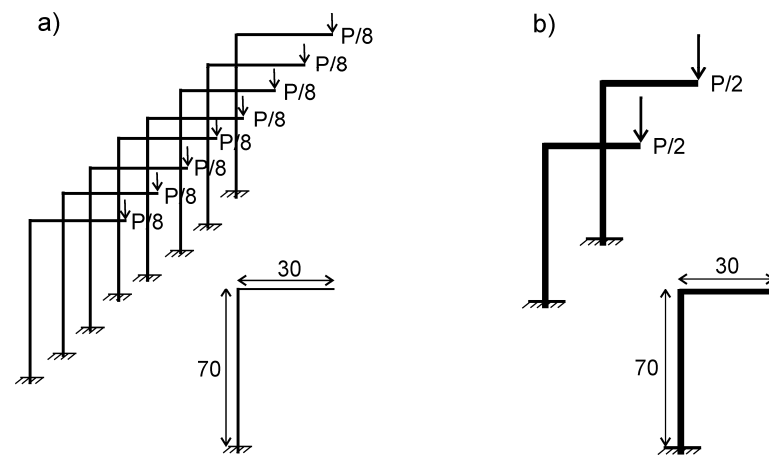


Figure 5. Eight-to-two aggregation of loaded Γ -frames; (a) non-aggregated structure; (b) aggregated structure.

The loading force applied to each of the non-aggregated Γ -frames in Figure 5a is $P/8$, while the loading force applied to each of the aggregated Γ -frames in Figure 5b is $P/2$. The total loading force for both structures was chosen to be the same—equal to $P = 24$ N and the Young modulus of the material for the frames was chosen to be 210 GPa. Table 3 summarises the results related to the maximum tensile stress and deflections related to the non-aggregated and aggregated Γ -frames. All calculations have been produced through standard techniques from stress analysis, and to conserve space, details have been omitted.

Table 3. Results for the maximum stress and deflection for the non-aggregated and aggregated Γ -frames.

	Non-Aggregated	Aggregated
Maximum stress	920.56 MPa	462.18 MPa
Maximum deflection	20.95 mm	5.23 mm

From the results for the loaded Γ -frames in Table 3, we can conclude that for the same volume of material, the aggregated structure was characterised with significantly smaller maximum stress and deflection. This is another confirmation of the validity of the aggregation method.

6. Experimental Verification

In all conducted experiments, a digital dynamometer capturing the applied load was used, with a range (0–50 N) and measurement accuracy of 1%. The displacement was captured using a digital depth gauge with a measurement range 0–80 mm and measurement precision 0.01 mm. In all conducted experiments, the experimental verification of the aggregation method was conducted using music wire with diameters of 1 mm and 2 mm and a Young’s modulus 179 GPa. The wire diameters were selected in such a way that the total cross-sectional area of two wires of diameter 2 mm was exactly equal to the total cross-sectional area of eight wires of diameter 1 mm:

$$2 \times \frac{\pi \times 2^2}{4} = 8 \times \frac{\pi \times 1^2}{4} = 2\pi \text{ mm}^2$$

6.1. Configuration of the Experimental Equipment for Cantilevered Structures

The experimental verification of the proposed aggregation method on simply supported beams was conducted using rods of music wire with diameters of 1 mm and 2 mm. A cantilever beam, labelled as ‘1’ and made from music wire, was securely anchored in

the vice, labelled as '2' (Figure 6). The beam's deflection was controlled by a digital depth gauge, labelled as '4', while the load applied to the free end of the beam was quantified using a digital dynamometer, labelled as '3'. The digital depth gauge '4' can be effortlessly repositioned horizontally, along the ferromagnetic rail '5', thanks to the magnetic catches integrated into the gauge's legs. The length L of the cantilever beam was 40 mm for both diameters of the music wire. The beam deflection was specified to be exactly 2 mm, and the loading force at this deflection was recorded. During the experiments, all deformations remained in the elastic region.

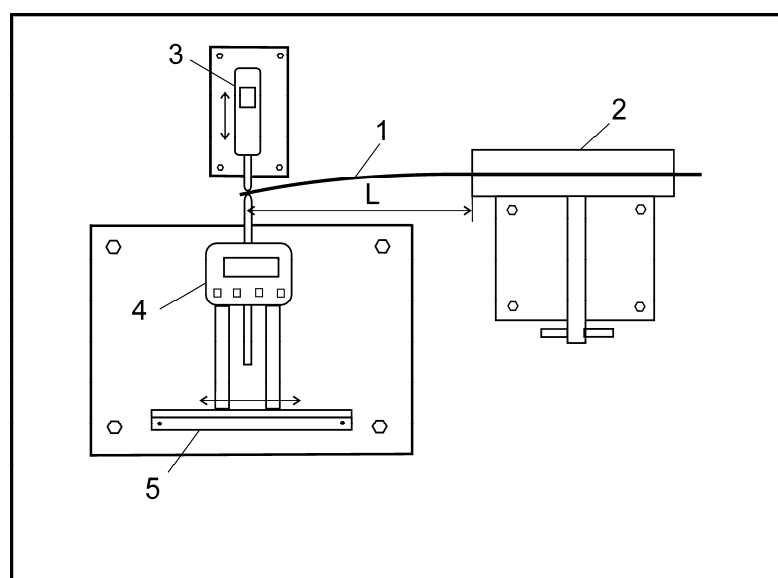


Figure 6. Configuration of the experimental equipment for cantilever beams: '1'—cantilever beam, '2'—vice, '3'—digital dynamometer, '4'—digital depth gauge, '5'—ferromagnetic rail.

6.2. Experimental Results for Cantilever Beams

For the music wire of 2 mm diameter, the average recorded force to reach 2 mm deflection of the free end was 13.16 N, while for the wire of 1 mm diameter, the average recorded force to reach 2 mm deflection of the free end was 0.85 N. Consequently, if uniformly loaded, two beams of 2 mm diameter will carry a total load of $2 \times 13.16 = 26.32$ N, while eight beams of 1 mm diameter will carry a total load of $8 \times 0.85 = 6.8$ N.

6.3. Configuration of the Experimental Equipment for Simply Supported Beams

The experimental verification of the proposed aggregation method on simply supported beams was conducted using rods of music wire with diameters of 1 mm and 2 mm. The simply supported beam labelled as '1' was securely positioned on the rolling supports '2' (Figure 7). The deflection of the simply supported beam '1' was measured by a digital depth gauge '4', while the load applied in the middle of the simply supported beam '1' was measured by the digital dynamometer '3'. The distance between the supports '2' was 80 mm for both diameters of the music wire, and the concentrated load from the push-dynamometer 3 was applied in the middle of the beam at a distance of 40 mm from the supports '2'. Again, the beam deflection in the middle was specified to be exactly 2 mm, and the loading force at this deflection was recorded. During the experiment, all deformations remained in the elastic region.

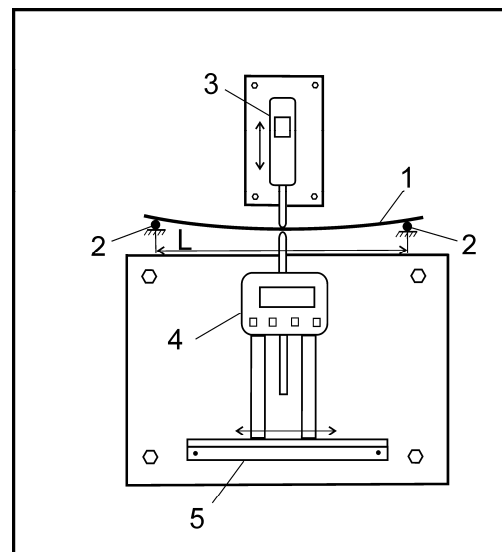


Figure 7. Configuration of the experimental equipment for simply supported beams: '1'—simply supported beam, '2'—supports, '3'—digital dynamometer, '4'—digital depth gauge, '5'—ferromagnetic rail.

6.4. Experimental Results for Simply Supported Beams

For the music wire of 1 mm diameter, the average recorded force to reach 2 mm deflection in the middle was 1.68 N, while for the music wire of 2 mm diameter, the average recorded force was 26.4 N.

Consequently, two uniformly loaded beams of 2 mm diameter will support a total load of $2 \times 26.4 = 52.8$ N while eight uniformly loaded beams of 1 mm diameter will support a total load of $8 \times 1.68 = 13.44$ N. The results from the experimental study related to cantilevered and simply supported beams are summarised in Table 4 and confirm that aggregation significantly increases the load-bearing capacity of structures subjected to bending.

Table 4. Maximum load (N) until 2 mm deflection for 8 non-aggregated versus 2 aggregated cantilever and simply supported beams.

	8 Non-Aggregated Beams	2 Aggregated Beams
Cantilever beams	6.8 N	26.32 N
Simply supported beams	13.44 N	52.8 N

6.5. Configuration of the Experimental Equipment for Γ -Frames

The experimental verification of the proposed aggregation method on Γ -frames was also conducted using frames made of music wire with diameters of 1 mm and 2 mm. Again, the selected aggregation was eight-to-two, and the dimensions of the frames (in mm) are shown in Figure 8.

A Γ -frame, labelled as '1', was securely anchored in the vice '2' (Figure 8). The frame's deflection was controlled by a digital depth gauge '4', while the load applied was measured using the digital dynamometer '3'.

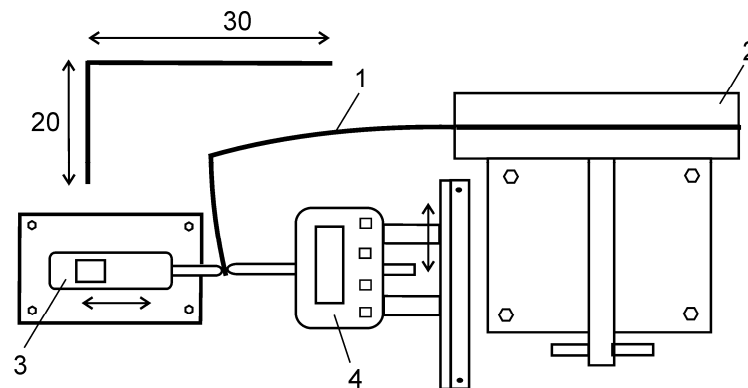


Figure 8. Experimental verification of the aggregation method using Γ -frames: '1'— Γ -frame, '2'—vice, '3'—digital dynamometer, '4'—digital depth gauge.

6.6. Experimental Results for Γ -Frames

The selected total bending load on the aggregated and non-aggregated Γ -frame was the same—equal to 8 N—and the deflection at this total load was measured. Because of the uniform loading, each element of the non-aggregated structure (eight frames) was effectively loaded with 1 N force, while each element of the aggregated structure (two frames) was loaded with 4 N ($8 \times 1 \text{ N} = 2 \times 4 \text{ N} = 8 \text{ N}$). The measured deflections from the experiments with the Γ -frames are summarised in Table 5. Based on the conducted measurements, it can be concluded that the deflections of the aggregated structure are significantly smaller than those of the non-aggregated structure. This confirms that aggregation increases the load-bearing capacity of structures subjected to bending.

Table 5. Maximum deflection for 8 non-aggregated Γ -frames versus 2 aggregated Γ -frames.

	8 Non-Aggregated Γ -Frames	2 Aggregated Γ -Frames
Deflection	1.59 mm	0.4 mm

6.7. Applications

Here is a list of possible applications of load-bearing elements loaded in bending that can benefit from aggregation:

- Steel beams supporting a distributed load, such as a floor in a building.
- Wooden joists arranged side by side to support the weight of a flooring system.
- Console I-beams installed in parallel to bear the load of a structure.
- I-beams installed in parallel to bear the load of a walkway or bridge.
- Reinforced concrete beams supporting the weight of a suspended parking deck.
- Parallel frames carrying the load of a prefabricated modular structure.
- Deck joists arranged uniformly to provide support for an outdoor decking system.

Simple application examples of non-aggregated and aggregated supporting structures are shown in Figure 9a and Figure 9b, respectively. The six-to-four aggregation in Figure 9a and the four-to-two aggregation in Figure 9b consists of reducing the number of loaded elements and increasing their cross sectional area accordingly. This operation substantially reduces the volume of material required to construct the supporting structures.

It needs to be pointed out that in conducting aggregation, the structural safety considerations should always apply. If failure of any of the aggregated elements induces collapse of the entire structure and the consequences of structural collapse are severe, the non-aggregated structure may be safer than the aggregated structure.

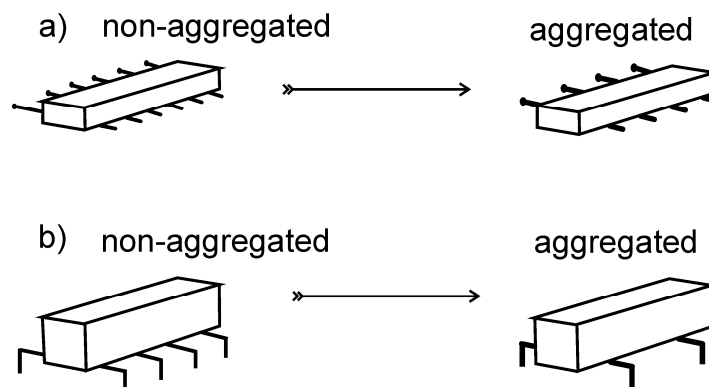


Figure 9. An application example of non-aggregated and aggregated structures: (a) a supporting structure built on console arms; (b) a supporting structure built on Π -frames.

The results reported in this paper are related to load-carrying elements with circular cross-sections loaded in bending. Simulations were also carried out (to be published elsewhere) with elements with square cross sections loaded in bending. The obtained results confirmed the proposed method of aggregation.

7. Conclusions

1. A powerful method for developing lightweight designs and improving the load-bearing capacity of common structures has been introduced, referred to as ‘the method of aggregation’. The essence of the proposed method is consolidating multiple elements loaded in bending into a reduced number of elements with larger cross sections but with a significantly smaller total volume of material.
2. General sub-additive and super-additive inequalities have been proposed and proved under a set of sufficient conditions. The proposed inequalities provide the theoretical basis for the method of aggregation related to developing lightweight designs and increasing the load-bearing capacity of structures loaded in bending.
3. The proposed sub-additive inequality compares the minimum volumes of material of structures necessary to support the same total bending load. The proposed super-additive inequality compares the load-bearing capacities of competing structures at the same total volume of material used for building the structures.
4. It has been demonstrated that aggregating multiple load-carrying cantilever beams and simply supported beams with circular cross-sections into a smaller number of beams with larger cross sections, supporting the same total load, leads to a very big reduction of the minimum necessary volume of material for the structure.
5. It has also been demonstrated that consolidating elements with circular cross-sections loaded in bending into a reduced number of elements, but with the same total volume of material, leads to a very big increase of the load-bearing capacity of the structure.
6. The validity of the proposed aggregation method has been confirmed experimentally on cantilever beams, simply supported beams, and Γ -frames with circular cross-sections.

Funding: This research received no external funding.

Data Availability Statement: Data are contained within the article.

Conflicts of Interest: The author declares no conflict of interest.

Appendix A. Proof of Inequality (1) in the General Case of Unequal x_i and y_i

Proof of inequality (1) for unequal x_i and y_i .

Let the conditions:

$$\begin{aligned} x_1 &\geq y_1; x_1 \geq y_2; \dots; x_1 \geq y_n \\ x_2 &\geq y_1; x_2 \geq y_2; \dots; x_2 \geq y_n \\ \dots & \\ x_m &\geq y_1; x_m \geq y_2; \dots; x_m \geq y_n \end{aligned} \tag{A1}$$

and the condition:

$$\sum_{i=1}^m x_i = \sum_{i=1}^n y_i \tag{A2}$$

be fulfilled.

Because $m < n$, it can be assumed that the left- and right-hand side of (1) have the same number of n terms, where $x_{m+1} = x_{m+2} = \dots = x_n = 0$. Without loss of generality, it can be assumed that

$$x_1 \geq x_2 \geq \dots \geq x_n \tag{A3}$$

$$y_1 \geq y_2 \geq \dots \geq y_n \tag{A4}$$

are fulfilled. Considering (A1), (A3), and (A4), the following majorization property can be established:

$$\begin{aligned} x_1 &\geq y_1; x_1 + x_2 \geq y_1 + y_2; \dots; \\ x_1 + x_2 + \dots + x_{n-1} &\geq y_1 + y_2 + \dots + y_{n-1}; \\ x_1 + x_2 + \dots + x_n &= y_1 + y_2 + \dots + y_n \end{aligned} \tag{A5}$$

Next, if, for any i , $x_i = y_i$, then the inequality (1) will not be affected if x_i and y_i are removed. As a result, without loss of generality, it can be assumed that $x_i \neq y_i$, for all i .

Consider the slope of the secant $\frac{ax^p - ay^p}{x - y}$ through the points (x, ax^p) and (y, ay^p) . The power law function $z = ax^p$ ($z = ay^p$) is concave and monotonically increasing function in x , and also considering conditions (A3) and (A4), this implies that the following property holds (see Figure A1):

$$k_i = \tan(\alpha) = \frac{ax_i^p - ay_i^p}{x_i - y_i} < \frac{ax_{i+1}^p - ay_{i+1}^p}{x_{i+1} - y_{i+1}} = k_{i+1} = \tan(\beta) \tag{A6}$$

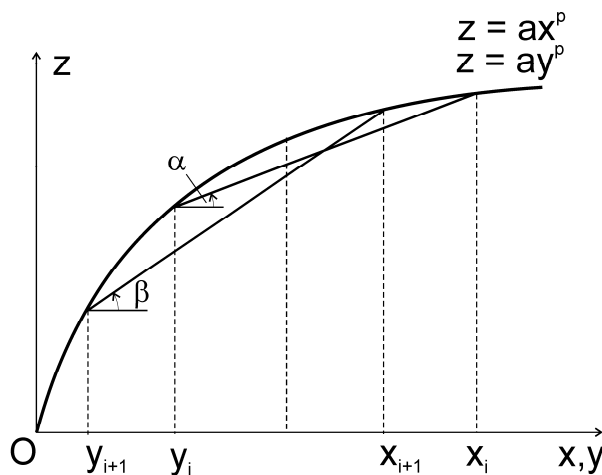


Figure A1. The key property (A6) for the concave power law function $z = ax^p$ ($z = ay^p$).

Let $X_0 = Y_0 = 0$ and $X_i = x_1 + x_2 + \dots + x_i$, $Y_i = y_1 + y_2 + \dots + y_i$, $i = 1, \dots, n$

From the majorization property (A5), it follows that $X_i \geq Y_i$ for $i = 1, \dots, n - 1$ and $X_n = Y_n$. Proving inequality (1) is equivalent to proving the inequality $\sum_{i=1}^n [ax_i^p - ay_i^p] < 0$.

From (A6), it follows that:

$$\sum_{i=1}^n [ax_i^p - ay_i^p] = \sum_{i=1}^n k_i(x_i - y_i) \tag{A7}$$

Since $x_i = X_i - X_{i-1}$ and $y_i = Y_i - Y_{i-1}$, the sum in the right-hand side of (A7) can be presented as:

$$\sum_{i=1}^n k_i(x_i - y_i) = \sum_{i=1}^n k_i[X_i - X_{i-1} - (Y_i - Y_{i-1})] = \sum_{i=1}^n k_i(X_i - X_{i-1}) - \sum_{i=1}^n k_i(Y_i - Y_{i-1}) \tag{A8}$$

In turn, the sum in the right-hand side of Equation (A8) can be presented as:

$$\begin{aligned} \sum_{i=1}^n k_i(X_i - X_{i-1}) - \sum_{i=1}^n k_i(Y_i - Y_{i-1}) &= k_1(X_1 - Y_1) + k_2(X_2 - Y_2) + k_3(X_3 - Y_3) + \dots + k_n(X_n - Y_n) \\ &\quad - k_1(X_0 - Y_0) - k_2(X_1 - Y_1) - k_3(X_2 - Y_2) - \dots - k_n(X_{n-1} - Y_{n-1}) \end{aligned}$$

As a result, the right-hand side of Equation (A8) becomes:

$$\sum_{i=1}^n k_i(X_i - X_{i-1}) - \sum_{i=1}^n k_i(Y_i - Y_{i-1}) = k_n(X_n - Y_n) - k_1(X_0 - Y_0) + \sum_{i=1}^{n-1} (k_i - k_{i+1})(X_i - Y_i)$$

Considering that $k_n(X_n - Y_n) = 0$, $k_1(X_0 - Y_0) = 0$, the right-hand side of Equation (A8) becomes:

$$\sum_{i=1}^n k_i(X_i - X_{i-1}) - \sum_{i=1}^n k_i(Y_i - Y_{i-1}) = 0 - 0 + \sum_{i=1}^{n-1} (k_i - k_{i+1})(X_i - Y_i)$$

As a result, the relationship $\sum_{i=1}^n k_i(x_i - y_i) = \sum_{i=1}^{n-1} (k_i - k_{i+1})(X_i - Y_i)$ has been established. Since $X_i - Y_i \geq 0$ and $k_i - k_{i+1} < 0$, it follows that $\sum_{i=1}^n k_i(x_i - y_i) < 0$, which proves inequality (1).

The truth of inequality (3) can be established by a very similar reasoning.

Appendix B. Proof of Inequality (1) in the Special Case of Equal x_i and y_i

Consider the special case of equal x_i and y_i :

$$\begin{aligned} x_1 = x_2 = \dots = x_m = z/m \text{ and } y_1 = y_2 = \dots = y_n = z/n \\ \sum_{i=1}^m x_i = z, \sum_{i=1}^m y_i = z, 0 < p < 1, \end{aligned}$$

In this case, inequality (1) can be proved by substituting $x_i = z/m$ and $y_i = z/n$ which results in the equivalent inequality:

$$m \times a(z/m)^p < n \times a(z/n)^p \tag{A9}$$

Proving the last inequality is equivalent to proving the inequality

$$az^p(n^{1-p} - m^{1-p}) > 0 \tag{A10}$$

The left-hand side of inequality (A10) is always positive because $n^{1-p}/m^{1-p} = (n/m)^{1-p} > 1$ if $n > m$ and $0 < p < 1$. From this, it follows that if $m < n$ and $0 < p < 1$, then $n^{1-p} - m^{1-p} > 0$, which completes the proof of inequality (A10) and the equivalent inequalities (A9) and (1).

The truth of inequality (3) for equal x_i and y_i can be established by a very similar reasoning, and the details will be omitted.

References

1. Fink, A.M. An essay on the history of inequalities. *J. Math. Anal. Appl.* **2000**, *249*, 118–134. [[CrossRef](#)]
2. Netzer, T.; Plaumann, D. *Geometry of Linear Matrix Inequalities: A Course in Convexity and Real Algebraic Geometry with a View towards Optimization*; Birkhauser: Basel, Switzerland, 2023.
3. Bechenbach, E.; Bellman, R. *An Introduction to Inequalities*; The L.W. Singer Company: New York, NY, USA, 1961.

4. Cvetkovski, Z. *Inequalities: Theorems, Techniques and Selected Problems*; Springer: Berlin/Heidelberg, Germany, 2012.
5. Marshall, A.W.; Olkin, I.; Arnold, B.C. *Inequalities: Theory of Majorization and Its Applications*, 2nd ed.; Springer Science and Business Media: New York, NY, USA, 2010.
6. Steele, J.M. *The Cauchy-Schwarz Master Class: An Introduction to the Art of Mathematical Inequalities*; Cambridge University Press: New York, NY, USA, 2004.
7. Hardy, G.; Littlewood, J.E.; Polya, G. *Inequalities*; Cambridge University Press: New York, NY, USA, 1999.
8. Sedrakyan, H.; Sedrakyan, N. *Algebraic Inequalities*; Springer: Cham, Switzerland, 2010.
9. Su, Y.; Xiong, B. *Methods and Techniques for Proving Inequalities*; World Scientific Publishing: Singapore, 2016.
10. Xie, M.; Lai, C.D. On Reliability Bounds via Conditional Inequalities. *J. Appl. Probab.* **1998**, *35*, 104–114. [[CrossRef](#)]
11. Makri, F.S.; Psillakis, Z.M. Bounds for Reliability of k-within Two-Dimensional Consecutive-r-Out-of-n Failure Systems. *Microelectron. Reliab.* **1996**, *36*, 341–345. [[CrossRef](#)]
12. Hill, S.D.; Spall, J.C.; Maranzano, C.J. Inequality-Based Reliability Estimates for Complex Systems. *Nav. Res. Logist.* **2013**, *60*, 367–374. [[CrossRef](#)]
13. Berg, V.D.; Kesten, H. Inequalities with Applications to percolation and reliability. *J. Appl. Probab.* **1985**, *22*, 556–569. [[CrossRef](#)]
14. Kundu, C.; Ghosh, A. Inequalities Involving Expectations of Selected Functions in Reliability Theory to Characterize Distributions. *Commun. Stat. Theory Methods* **2017**, *46*, 8468–8478. [[CrossRef](#)]
15. Dohmen, K. Improved Inclusion-Exclusion Identities and Bonferroni Inequalities with Reliability Applications. *SIAM J. Discret. Math.* **2002**, *16*, 156–171. [[CrossRef](#)]
16. Todinov, M.T. Reverse Engineering of Algebraic Inequalities for System Reliability Predictions and Enhancing Processes in Engineering. *IEEE Trans. Reliab.* **2023**. [[CrossRef](#)]
17. Alsina, C.; Nelsen, R.B. *Charming Proofs: A Journey into Elegant Mathematics*; The Mathematical Association of America: Washington, DC, USA, 2010.
18. Walton, D.; Moztarzadeh, H. Design and Development of an Additive Manufactured Component by Topology Optimization. *Procedia CIRP* **2017**, *60*, 205–210. [[CrossRef](#)]
19. Chen, L.; Zhang, Y.; Chen, Z.; Xu, J.; Wu, J. Topology optimization in lightweight design of a 3D-printed flapping-wing micro aerial vehicle. *Chin. J. Aeronaut.* **2020**, *33*, 3206–3219. [[CrossRef](#)]
20. Rosenthal, S.; Maaß, F.; Kamaliev, M.; Hahn, M.; Gies, S.; Tekkaya, A.E. Lightweight in automotive components by forming technology. *Automot. Innov.* **2020**, *3*, 195–209. [[CrossRef](#)]
21. Mandolini, M.; Pradel, P.; Cicconi, P. Design for Additive Manufacturing: Methods and Tools. *Appl. Sci.* **2022**, *12*, 6548. [[CrossRef](#)]
22. Yang, L.; Harrysson, O.L.A.; Cormier, D.; West, H.; Zhang, S.; Gong, H.; Stucker, B. Design for Additively Manufactured Lightweight Structure: A Perspective, Solid Freeform Fabrication. In Proceedings of the 27th Annual International Solid Freeform Fabrication Symposium—An Additive Manufacturing Conference, Austin, TX, USA, 8–10 August 2016.
23. Budynas, R.G.; Nisbett, J.K. *Shigley's Mechanical Engineering Design*, 10th ed.; McGraw-Hill Education: New York, NY, USA, 2015.
24. Collins, J.A. *Mechanical Design of Machine Elements and Machines*; John Wiley & Sons, Inc.: New York, NY, USA, 2003.
25. Budynas, R.G. *Advanced Strength and Applied Stress Analysis*, 2nd ed.; McGraw-Hill: New York, NY, USA, 1999.
26. Hearn, E.J. *Mechanics of Materials*, 2nd ed.; Butterworth-Heinemann: Oxford, UK, 1985; Volume 1.
27. Gere, J.M.; Timoshenko, S.P. *Mechanics of Materials*, 4th ed.; Stanley Thornes (Publishers) Ltd.: Surrey, UK, 1999.
28. Hibbeler, R. *Structural Analysis in SI Units*, Global ed.; Pearson: London, UK, 2019.
29. Podder, D.; Chatterjee, S. *An Introduction to Structural Analysis*; CRC Press: Boca Raton, FL, USA, 2022.
30. Wang, C. *Structural Reliability and Time-Dependent Reliability*; Springer Series in Reliability Engineering; Springer: Cham, Switzerland, 2020.
31. Kiureghian, A. *Structural and System Reliability*; Cambridge University Press: Cambridge, UK, 2022.
32. Yanga, K.-H.; Ashourb, A.F. Aggregate interlock in lightweight concrete continuous deep beams. *Eng. Struct.* **2011**, *33*, 136–145. [[CrossRef](#)]
33. Qiao, H.; Li, H. The discussion on optimization models of pure bending beam. *Int. J. Adv. Struct. Eng.* **2013**, *5*, 11. [[CrossRef](#)]

Disclaimer/Publisher's Note: The statements, opinions and data contained in all publications are solely those of the individual author(s) and contributor(s) and not of MDPI and/or the editor(s). MDPI and/or the editor(s) disclaim responsibility for any injury to people or property resulting from any ideas, methods, instructions or products referred to in the content.